Supporting Information

Fu et al. 10.1073/pnas.1323265111

SI Materials and Methods

Cell Culture and Differentiation. All cells used in this study were cultured at 37 °C under 5% (vol/vol) CO_2. Primary mouse myoblasts were isolated as previously described (1) and were grown on BD Matrigel-coated plates. The C2C12 cell line and human skeletal myoblasts (SkM) were purchased from ATCC and Lonza, respectively. Five embryonal RMS (A204, RD, RD12, RD18, and RH36) and five alveolar RMS (RH4, RH18, RH28, RH30, and RH41) cell lines were studied. A204 and RD were purchased from ATCC, RH4 and RH30 were obtained from M. Hatley (St. Jude Children's Research Hospital, Memphis, TN), RH18, RH28, RH36, and RH41 were from G. Germain (St. Jude Children's Research Hospital), and RD12 and RD18 were from P.-L. Lollini and L. Landuzzi (University of Bologna, Bologna, Italy).

Before differentiation, cells were cultured in growth medium (GM) on Matrigel-coated surfaces (plates, coverslips, or Lab-Tek chamber slides). C2C12 cells were grown to confluence, and primary mouse myoblasts and SkM were grown to ∼75% confluence. Because of the rapid proliferation of most RMS cell lines, the RMS cells were grown to 40–50% confluence before differentiation. To induce differentiation, cells were switched to differentiation medium (DM). For C2C12 and RMS cell lines, GM is DMEM supplemented with 10% (vol/vol) FBS, and DM is DMEM with 2% (vol/vol) horse serum (HS). For primary mouse myoblasts, DMEM/F10 (1:1) containing 20% (vol/vol) FBS was used as GM, and DMEM/5% (vol/vol) HS was used as DM. GM for SkM cells was SkGM-2 medium (Lonza), and DMEM/F12 (1:1) with 2% (vol/vol) HS was used as DM.

RNA Interference and Retroviral Infection. RNAi in myoblasts was performed as previously described (2). Briefly, a modified version of the microRNA (miRNA) retroviral expression system was used to silence specific genes, and the miRNA targeting sequences were designed through RNAi Codex database (http://cancan.cshl.edu/cgi-bin/Codex/Codex.cgi). The scrambled sequence and sequences targeting Cep290, IFT80, and IFT88 are as follows: Scramble (CAATTCTCCGAACGTGTCACGT), Cep290-1 and Cep290-2 (CACTATGAACTTGTTCAATATC and CAGAGAGGAGCAAAGAGAA), IFT80-1 and IFT80-2 (CCTCTTCAACCAAATGCTA and GCAAACAGCTCATCATTAA), and IFT88-1 and IFT88-2 (CAGAACATTGGAATCACAT and CTGTGAACTCGGATAGATA). The IFT88 cDNA from C. Desdouets (Faculté de médecine R. Descartes, Paris) (3) was subcloned into the pBabe vector, and IFT88 RNAi-resistant constructs were generated by introducing silent point mutations to the miRNA target sequences: CAGAACATAGGTATCACAT and CTGTGAACAGTGATAGATA (mutated nucleotides underlined).

For viral infections, retroviral particles were produced in Phoenix-Eco cells as previously described (2, 4). C2C12 cells or primary mouse myoblasts were infected at least three times with viral supernatants supplemented with 8 μg/mL polybrene, and puromycin was subsequently added at 2–6 μg/mL to select against nontransduced cells before further analysis.

RNA Isolation and Quantitative Real-Time PCR. RNA was isolated with TRIzol (Invitrogen) according the manufacturer's instructions. Quantitative real-time PCR (qRT-PCR) was performed as previously described (5). Two hundred fifty nanograms of total RNA was used per reverse transcriptase reaction using the Verso cDNA synthesis kit (Thermo Scientific). qRT-PCR analysis was performed using the SYBR green method, and relative gene expression was analyzed as described previously (6). For mouse cells, *Sparc* was used as reference gene, and *GAPDH* was used as the reference gene for human cells. All primer sequences are available upon request.

Antibodies, Immunofluorescence, and Microscopic Analysis. The antibodies used in this study include the following: anti-myosin heavy chain (MHC) (Hybridoma bank), anti-Gli3 [6F5; gift from Suzie Scales (Genetech, South San Francisco, CA)] (7), anti-Gli2 (sc-28674; Santa Cruz), anti-α-tubulin (T5168; Sigma-Aldrich), anti-acetylated tubulin (T7451; Sigma-Aldrich), anti-γ-tubulin (T5192; Sigma), anti-GT335 (ASB-ARP45817-T100; Axxora), anti-K_i-67 (ab15580; Abcam), anti-Cep290 (A301-659A; Bethyl), anti-CP110 (8), anti-dynein (sc-9115; Santa Cruz), anti-IFT88 (13967-1-AP; Proteintech), anti-detyrosinated tubulin (AB3201; Chemicon), anti-phospho-Histone H3 (Ser10) (MC463; Upstate), and anti-Rab8 (610844; BD Bioscience).

Cells grown on coverslips or chamber slides were fixed in methanol at −20 °C before being processed for immunofluorescence. The primary and secondary antibodies were diluted in PBS containing 3% (wt/vol) BSA and 0.1% (vol/vol) Triton X-100. After incubation with primary antibodies for 1 to 2 h at room temperature, coverslips were washed in PBS and then processed for incubation with secondary antibodies for 1 h at room temperature. Coverslips were washed with PBS, and the DNA was stained with 1 μg/mL DAPI. The samples were mounted with ProLong Gold Antifade reagent (Life Technologies).

Fixed paraffin-embedded RMS tissue arrays were purchased from US Biomax. Two different arrays contained eight normal skeletal muscle samples and 33 different patient samples: array 1, 18 cases; array 2, 24 cases. The slides were deparaffinized using standard procedures. Next, samples were processed in methanol containing 3% (vol/vol) H_2O_2 followed by antigen retrieval in 0.01 M citrate buffer (pH 6.0). Slides were blocked in PBS containing 3% (wt/vol) BSA and 0.4% (vol/vol) Triton X-100. The primary and secondary antibodies were diluted in PBS/3% (wt/vol) BSA/0.1% (vol/vol) Triton, and immunofluorescence was performed as for cultured cells. The clinical diagnoses of the three patients with primary cilia are shown (Table S1).

For microscopy, images were acquired with an Axiovert 200M microscope (Carl Zeiss) equipped with MetaMorph7 program (Molecular Devices). Alternatively, an LSM 510 microscope (Zeiss) with Zen software (Zeiss) was used. The quantification and measurement of fluorescence images were performed using ImageJ software.

Quantitative analyses of differentiation were performed in three ways: (*i*): differentiation index was calculated as the percentage of nuclei incorporated into MHC-positive cells as a function of total nuclei; (*ii*); relative MHC intensity, measured as the MHC fluorescence intensity per 10× microscopic field; (*iii*); fusion index, estimated as the percentage of nuclei in fused MHC-positive myotubes as a function of all nuclei in MHC-positive cells.

Flow Cytometry and Cell Cycle Analysis. Before flow cytometry, cells were washed in PBS and fixed with cold ethanol overnight at 4 °C. Propidium iodide with RNase A was used to stain the DNA at room temperature for 30 min. Flow cytometry was performed with a BD FACSCalibur Cell Analyzer. Cell cycle distributions were calculated using FlowJo software. 5-ethynyl-2′-deoxyuridine (EdU) incorporation was analyzed according to the manufacturer's instructions using the Click-iT Plus EdU Alexa Fluor 594 Imaging Kit (Life Technologies).

Statistical Analysis. The statistical significance of differences was calculated with a two-tailed Student *t* test. Differences were considered significant at $P < 0.05$.

1. Rando TA, Blau HM (1994) Primary mouse myoblast purification, characterization, and transplantation for cell-mediated gene therapy. *J Cell Biol* 125(6):1275–1287.
2. Asp P, Acosta-Alvear D, Tsikitis M, van Oevelen C, Dynlacht BD (2009) E2f3b plays an essential role in myogenic differentiation through isoform-specific gene regulation. *Genes Dev* 23(1):37–53.
3. Robert A, et al. (2007) The intraflagellar transport component IFT88/polaris is a centrosomal protein regulating G1-S transition in non-ciliated cells. *J Cell Sci* 120(Pt 4):628–637.
4. Acosta-Alvear D, et al. (2007) XBP1 controls diverse cell type- and condition-specific transcriptional regulatory networks. *Mol Cell* 27(1):53–66.
5. van Oevelen C, et al. (2010) The mammalian Sin3 proteins are required for muscle development and sarcomere specification. *Mol Cell Biol* 30(24):5686–5697.
6. Livak KJ, Schmittgen TD (2001) Analysis of relative gene expression data using real-time quantitative PCR and the 2(-Delta Delta C(T)) Method. *Methods* 25(4):402–408.
7. Wen X, et al. (2010) Kinetics of hedgehog-dependent full-length Gli3 accumulation in primary cilia and subsequent degradation. *Mol Cell Biol* 30(8):1910–1922.
8. Chen Z, Indjeian VB, McManus M, Wang L, Dynlacht BD (2002) CP110, a cell cycle-dependent CDK substrate, regulates centrosome duplication in human cells. *Dev Cell* 3(3):339–350.

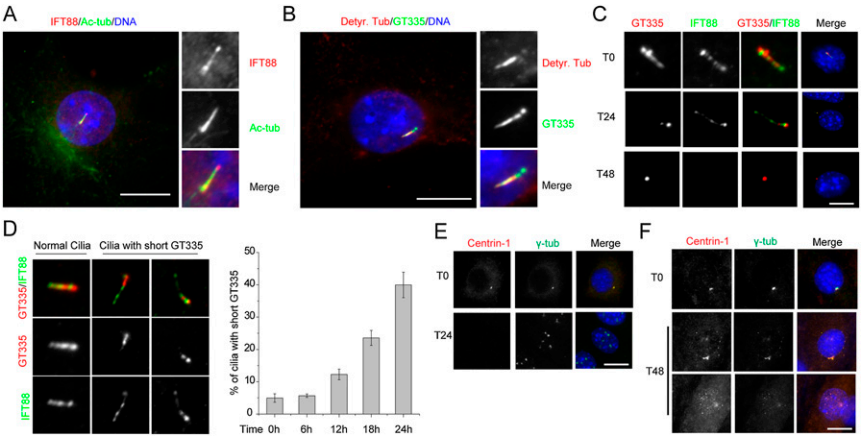

Fig. S1. Dynamic reorganization of primary cilia and centrosome proteins during differentiation. (*A* and *B*) Staining of various cilia markers in primary mouse myoblasts at T0. (*C*) Representative images showing cilia during differentiation from T0 to T48 in primary mouse myoblasts. (*D*) Quantification of the increase in primary cilia with truncated GT335 staining during transition from T0 to T24. (*E* and *F*) Images showing the reorganization of centrosomal proteins during differentiation in primary mouse myoblasts (*E*) and mouse C2C12 cells (*F*). (Scale bars, 10 μm.)

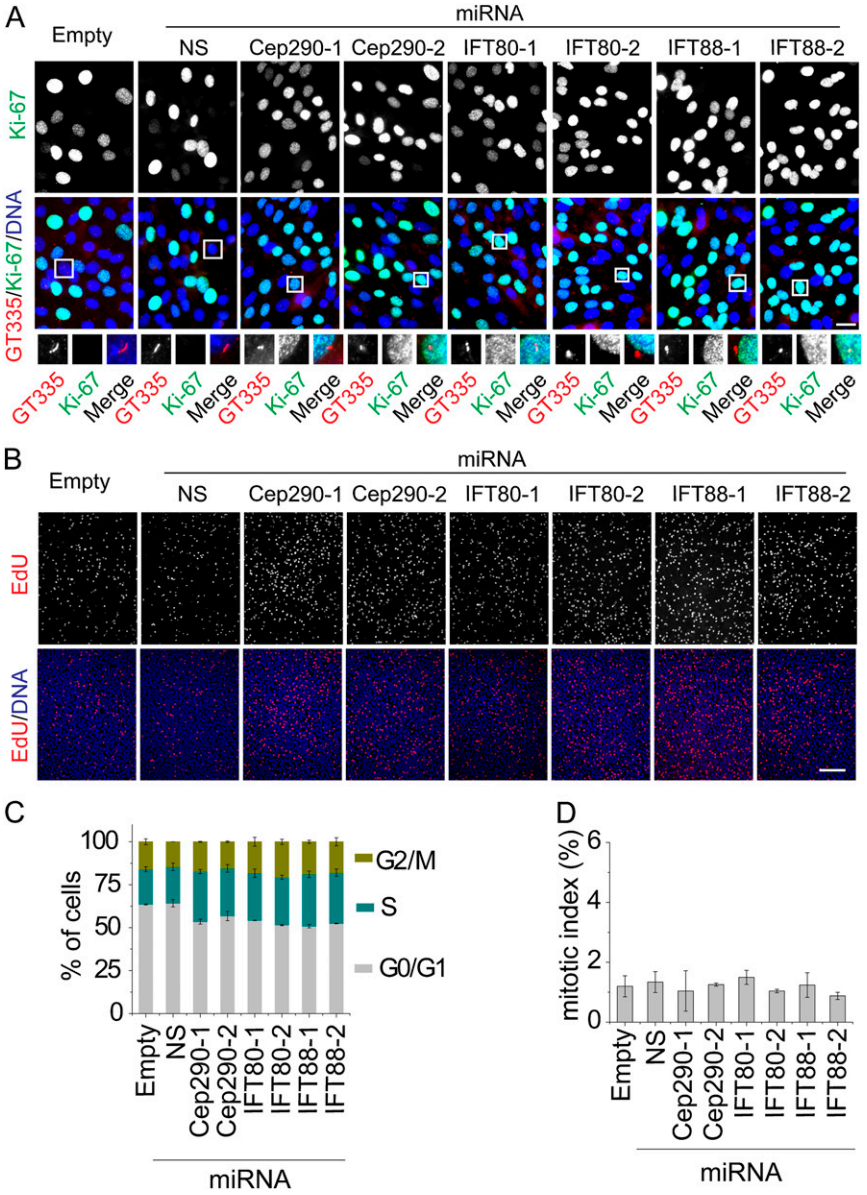

Fig. S2. Assembly of primary cilia regulates myoblast proliferation. (*A*) Representative immunofluorescence images of C2C12 cells treated with different miRNAs as indicated. Detection of cilia markers GT335, K_i-67, and DNA is presented. Magnified images of *Insets* (boxes) are shown. (Scale bar, 30 μm.) (*B*) Images showing EdU staining. (Scale bar, 200 μm.) (*C*) FACS analysis of C2C12 cells expressing different miRNAs. (*D*) Mitotic index of C2C12 cells detected by anti-phospho-histone H3 (Ser10) staining. Data are shown as mean ± SD.

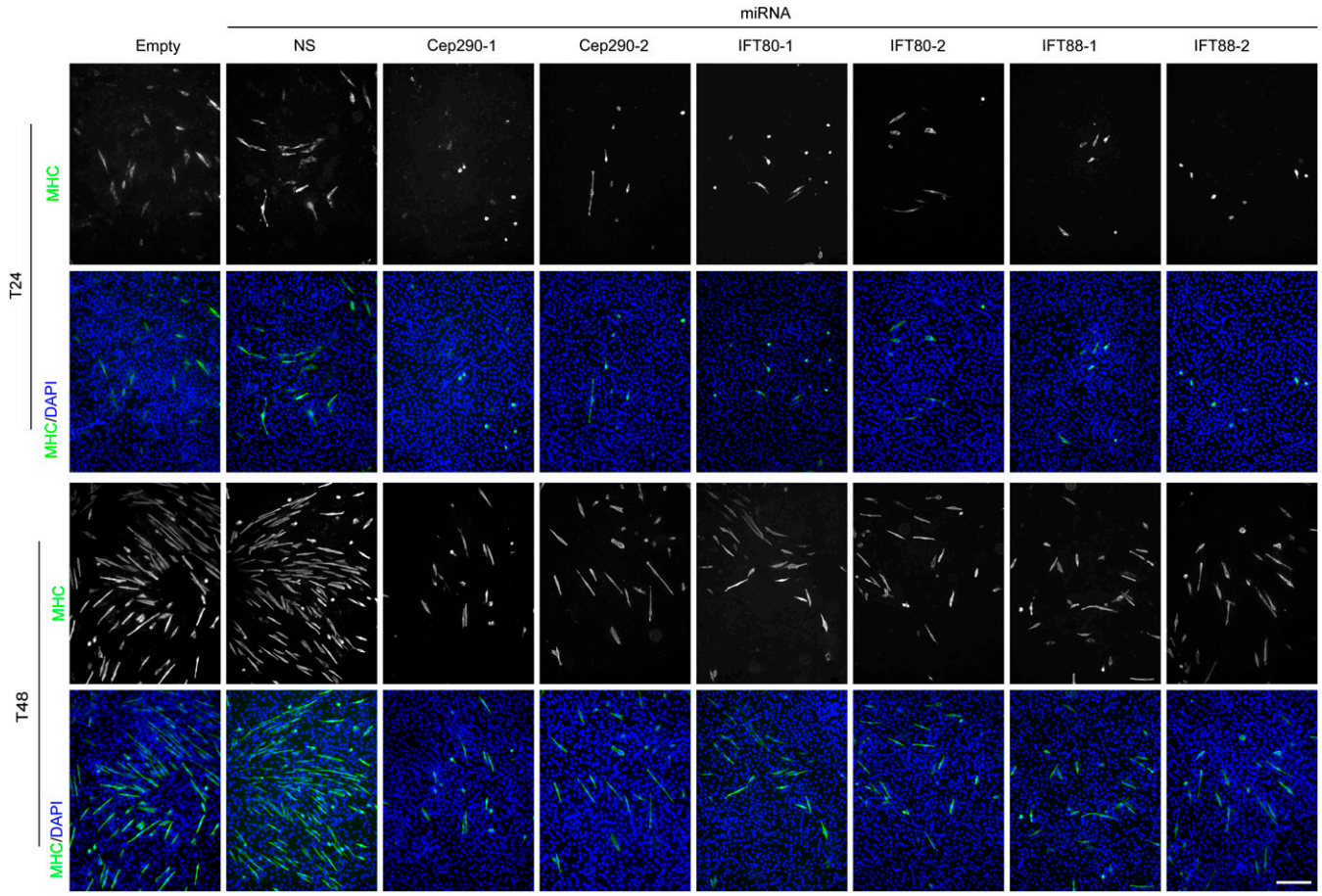

Fig. S3. Primary cilia regulate myoblast differentiation. The differentiation efficiency of C2C12 cells expressing distinct miRNAs was examined at T24 and T48 as indicated. Representative images are shown. (Scale bar, 200 μm.)

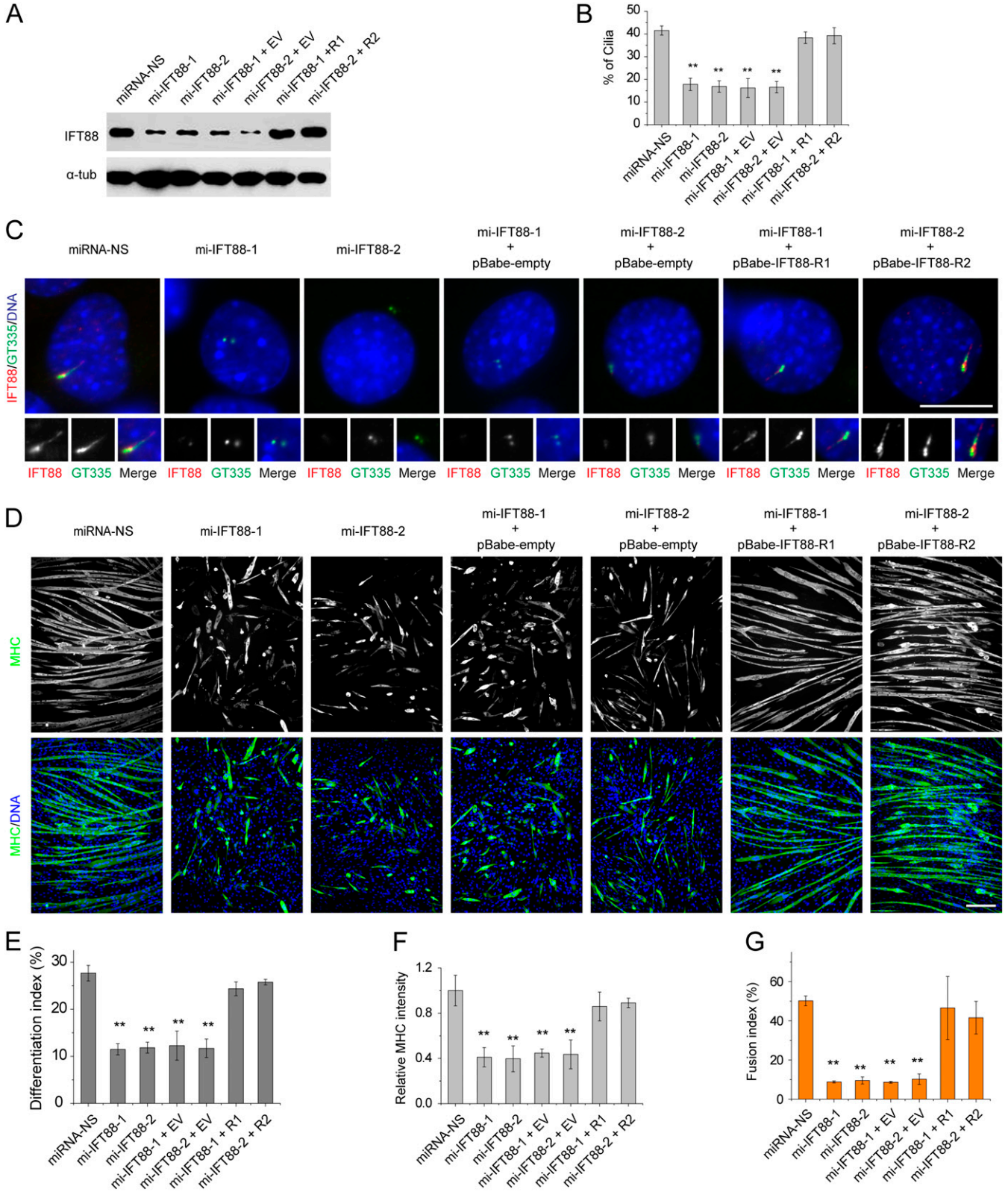

Fig. S4. Rescue of IFT88 knockdown by RNAi-resistant cDNAs. (*A*) Western blotting of IFT88 protein levels in C2C12 cells expressing miRNAs and miRNA-resistant constructs as indicated. EV, empty vector; R1 and R2, RNAi-resistant constructs. α-tubulin is shown as loading control. (*B*) Percentages of ciliated cells resulting from IFT88 silencing and rescue are shown. (*C*) Representative images of C2C12 cells stained with GT335 (green) and IFT88 (red). (Scale bar, 10 μm.) (*D*) Representative images of C2C12 cells after differentiation (T96) are shown. (Scale bar, 200 μm.) (*E*–*G*) Quantitative analysis of the differentiation index (*E*), relative MHC intensity (*F*), and fusion index (*G*) of C2C12 cells as in *D*. Error bars, ±SD. $^{**}P < 0.01$.

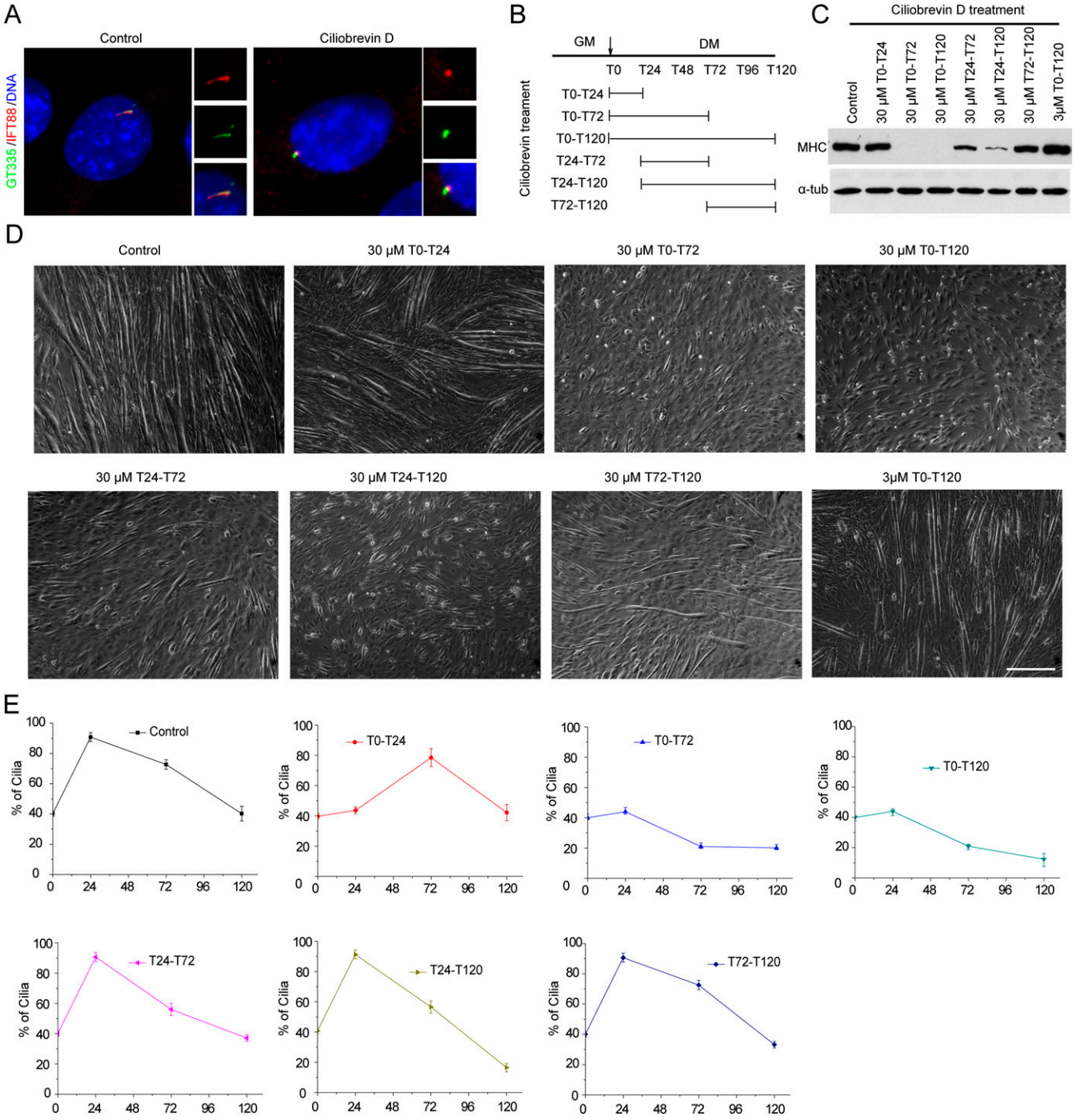

Fig. S5. Dynein inhibitor ciliobrevin D suppresses both cilia assembly and differentiation. (*A*) C2C12 cells were treated with ciliobrevin D, and representative immunofluorescence images of cilia are shown. The extent of ciliation in each treatment condition was assessed. (Scale bar, 10 μm.) (*B*) Experimental setup for ciliobrevin D treatment during different time intervals. (*C*) Western blots of indicated proteins at T120 after differentiation of C2C12 cells treated with ciliobrevin D. (*D*) Representative bright-field images of C2C12 cells after indicated treatments during differentiation. (Scale bar, 200 μm.) (*E*) Percentages of cilia during the time course for each 30 μM ciliobrevin D treatment. Error bars, ±SD.

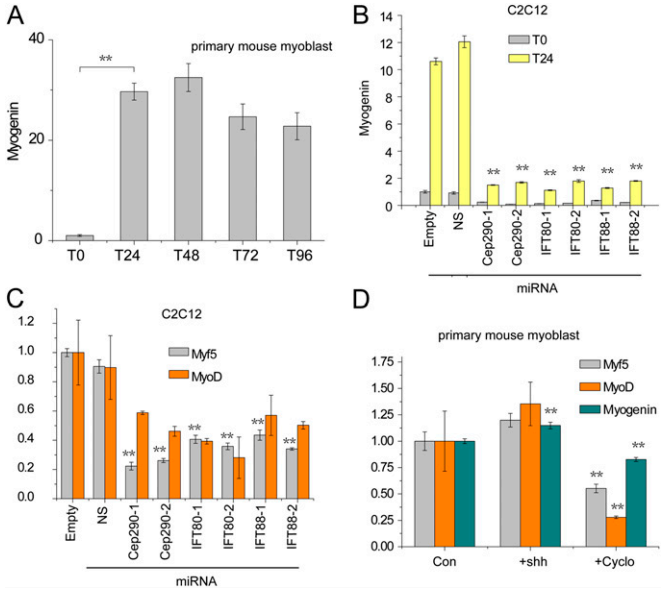

Fig. S6. Primary cilia regulate expression of myogenic transcription factors. (*A*) qRT-PCR analysis of myogenin mRNA levels in primary mouse myoblasts. (*B*) Myogenin expression in C2C12 cells depleted of ciliary proteins at T0 and T24 as indicated. (*C*) MyoD and Myf5 expression in C2C12 cells depleted of ciliary proteins at T0 are shown. (*D*) qRT-PCR detection of Myf5, MyoD, and myogenin in primary mouse myoblasts treated with sonic hedgehog (shh) or cyclopamine at T0 as indicated. Error bars, SEM. $^{**}P < 0.01$.

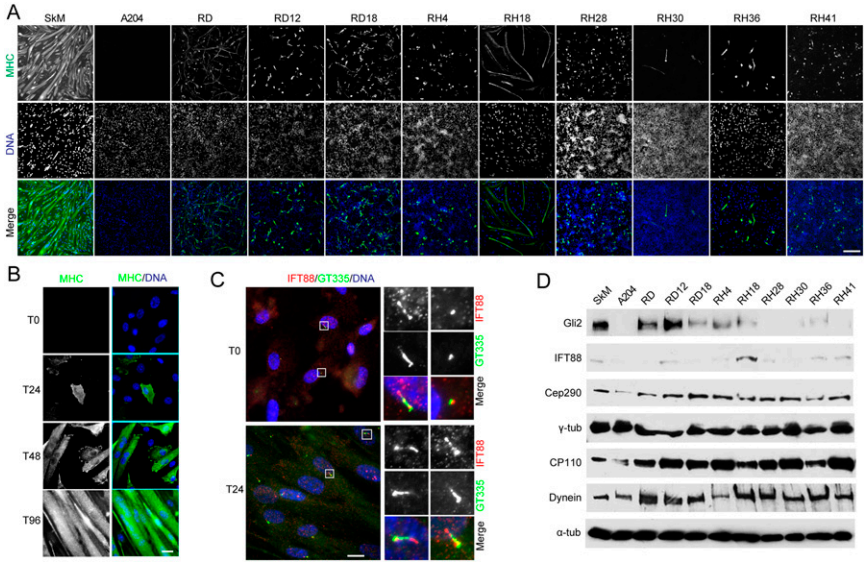

Fig. S7. Ciliogenesis and differentiation are deregulated in RMS cells. (*A*) Normal human skeletal myoblasts (SkM) and 10 RMS cell lines were induced to differentiate for 96 h, and representative images are shown. (Scale bar, 200 μm.) (*B* and *C*) Representative immunofluorescence images of SkM cells induced to differentiate and stained with indicated antibodies or DAPI (DNA) at indicated time points. (Scale bar, 10 μm.) (*D*) Western blot detection of indicated centrosomal/ciliary proteins in SkM and RMS cells.

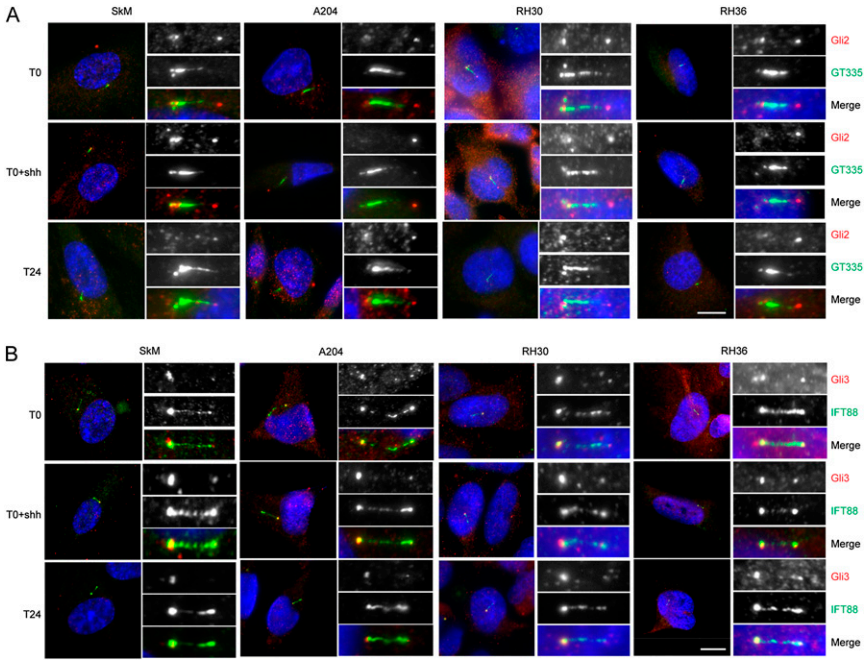

Fig. S8. Hedgehog components are deregulated in ciliated RMS cells. (*A*) Staining of Gli2 in SkM, A204, RH30, and RH36 cells with the conditions indicated. Gli2 shows localization at the ciliary tip and basal body. (*B*) Staining of Gli3 in RMS cells as indicated. Representative images are shown. Staining was considered negative at cilia when little or no staining at the cilium tip was observed. (Scale bar, 10 μm.)

Table S1. Clinical features of the three RMS patients with primary cilia

	Patient no.		
Parameter	Patient 1 (K4)	Patient 2 (G8)	Patient 3 (H1)
Found in array*	#2	#1	#1 and #2
Tissue type	Striated muscle	Striated muscle	Striated muscle
Sex	Male	Male	Male
Age, y	5	50	10
Pathology diagnosis	Alveolar RMS	Pleomorphic RMS	Alveolar RMS
Stage	—	IIA	IIB
TNM[†]	—	T1aN0M0 G2	T2aN0MO G2
Type	Malignant	Malignant	Malignant

*Eighteen patient samples in array #1 and 24 in array #2, with nine overlapping cases.

[†]TNM is a cancer staging system. T is the size and/or extent of the primary tumor, N is the amount of spread to nearby lymph nodes, and M indicates the presence of metastasis. G is the grade of cancer cell appearance compared with normal cells.